ELSEVIER

Neurobiology of Aging 33 (2012) 199.e1–199.e12

NEUROBIOLOGY OF AGING

www.elsevier.com/locate/neuaging

Aluminum induces neurodegeneration and its toxicity arises from increased iron accumulation and reactive oxygen species (ROS) production

Zhihao Wu[a], Yumei Du[a], Hua Xue[a], Yongsheng Wu[a], Bing Zhou[a,*]

[a] State Key Laboratory of Biomembrane and Membrane Biotechnology, School of Life Sciences, Tsinghua University, Beijing 100084, China

Received 8 February 2010; received in revised form 1 June 2010; accepted 21 June 2010

Abstract

The neurotoxicity of aluminum (Al) − the most abundant metal element on earth − has been known for years. However, the mechanism of Al-induced neurodegeneration and its relationship to Alzheimer's disease are still controversial. In particular, *in vivo* functional data are lacking. In a *Drosophila* model with chronic dietary Al overloading, general neurodegeneration and several behavioral changes were observed. Al-induced neurodegeneration is independent of β-amyloid or tau-associated toxicity, suggesting they act in different molecular pathways. Interestingly, *Drosophila frataxin* (*dfh*), which causes Friedreich's ataxia if mutated in humans, displayed an interacting effect with Al, suggesting Friedreich's ataxia patients might be more susceptible to Al toxicity. Al-treated flies accumulated large amount of iron and reactive oxygen species (ROS), and exhibited elevated SOD2 activity. Genetic and pharmacological efforts to reduce ROS or chelate excess Fe significantly mitigated Al toxicity. Our results indicate that Al toxicity is mediated through ROS production and iron accumulation and suggest a remedial route to reduce toxicity due to Al exposure.

Keywords: Al; AD (Alzheimer's disease); Iron dyshomeostasis; ROS

1. Introduction

Most cases of neurodegenerative diseases do not have obvious genetic origins; instead, they are sporadic and suspected to have environmental causes. Aluminum is the most abundant metal on earth and a well-known environmental neurotoxin. In the past decades, several human neurodegenerative diseases, such as Alzheimer's disease (AD) and amyotrophic lateral sclerosis (ALS)/Parkinsonism-dementia of Guam, were proposed to be related to Al overloading (Miu and Benga, 2006; Oyanagi, 2005; Savory et al., 2006).

However, for a long time, a potential role for Al neurotoxicity and its contribution to the pathogenesis of AD has been largely debated. Studies by different groups have yielded contradictory results. As a nonphysiological metal, Al is dispersed in different parts of the cell, including mitochondria, lysosomes and nucleus (Dobson et al., 1998). Al-caused toxicity is associated with multifaceted and complicated effects, such as inhibiting DNA repair system, changing the stability of DNA structure (Karlik et al., 1980; Lankoff et al., 2006), repressing PP2A activity (Walton, 2007), affecting the activity of antioxidant enzymes, disturbing cellular metal homeostasis especially that of iron (Fe) (Kim et al., 2007; Middaugh et al., 2005; Ward et al., 2001), enhancing reactive oxygen species (ROS) production (Khanna and Nehru, 2007; Kumar et al., 2009), interfering with mitochondrial functions (Kumar et al., 2008), and altering NF-κB, p53, JNK pathway to induce apoptosis (Savory et al., 1999; Savory et al., 2006). Nevertheless, the core mechanism of Al toxicity still remains unclear. In particular, it is unknown whether iron accumulation or ROS mediates Al toxicity, or they are just the consequence of cell damaging.

Several animal models have been developed to study the pathological and molecular changes induced by Al (Bertholf

* Corresponding author. Tel: +86 10 62795322; Fax: +86 10 62772253.
E-mail address: zhoubing@mail.tsinghua.edu.cn (B. Zhou).

0197-4580/$ – see front matter © 2012 Elsevier Inc. All rights reserved.
doi:10.1016/j.neurobiolaging.2010.06.018

et al., 1989; Drago et al., 2008; Klatzo et al., 1965). Due to the relative insensitivity of mice to Al neurotoxicity, rabbits are popularly used to study Al toxicity instead (Kihira et al., 2004; Yokel, 1989). Al-induced rabbit AD models displayed pathological hallmarks of AD, including neurodegeneration and neurofibrillary tangles, similar to those found in AD patients. However, other hallmarks of AD, such as neuritic plaques were not observed in the experimental animals (Savory et al., 2006).

Lack of genetic tools in rabbit models makes it particularly difficult to decipher the underlying molecular and cellular pathways involved in Al toxicity. The fruit fly *Drosophila melanogaster* has proven be a powerful platform with plenty of amenable genetic techniques to investigate the mechanism of human neurodegenerative diseases (Bilen and Bonini, 2005). In this study, we used a *Drosophila* model to investigate Al neurotoxicity. By feeding flies with $AlCl_3$, toxicity was observed as reported before (Massie et al., 1985). Typical neurological disorders, including reduced lifespan, loss of locomotion, tasting and learning abnormality, and degenerative vacuoles in the brain, were observed. Several models of human neurodegenerative diseases were tested for their interactions with Al. Neither β-amyloid peptide nor tau protein displayed synergistic effect with Al. *Frataxin* flies, on the contrary, were more sensitive to the toxic effect of Al. Reduction of either iron absorption or ROS generation by genetic methods or pharmacological interventions significantly mitigated Al toxicity, indicating that iron accumulation and ROS production play important roles in mediating Al toxicity.

2. Methods

2.1. Fly stock, culture media, reagents, and genetics

Fly stocks used for behavioral analyses were maintained in the standard cornmeal food, at 25 °C (except noted), 70% humidity, under a 12 hour light–dark cycle, and when noted, supplemented with appropriate chemicals as stated in each experiment. All reagents were from Sigma, Belgium unless specified otherwise.

The background stock (*220 2U*) used as the wild type flies in all the experiments is an isogenic line derived from a w^{1118} line repeatedly backcrossed to a Canton-S wild-type strain. *UAS-SOD1*, *UAS-SOD2*, *UAS-CAT* and *p[genomic-MitoCAT]* were from Dr A. Hilliker laboratory (Anderson et al., 2008). *UAS-FER1HCH*, *UAS-FER2LCH* and *UAS-FER1HCH, UAS-FER2FCH* were gifts from Dr. F. Missirlis laboratory (Missirlis et al., 2007). *dfh*-RNAi was from Dr Molto laboratory (Llorens et al., 2007). *UAS-Aβ42Arc* and *UAS-EGFP* was obtained from Dr Yi Zhong laboratory (Tsinghua University, China). *UAS-tauR406W* was generated by Dr M. Feany (Harvard University, USA) and a gift from Dr Bingwei Lu laboratory (Stanford University, USA). *Da-GAL4*, *actin-GAL4/Cyo* and *elav-GAL4* were stocks from Bloomington Stock Center (Indiana University, USA). To minimize differences in genetic backgrounds, before the assays all GAL4 lines and transgenic lines were outcrossed with *220 2U* for six generations.

2.2. Behavior assays

2.2.1. Survival assay

Twenty-five flies were placed in a food vial and raised with standard food and conditions (25 °C except in Fig. 1E, which was recorded in 29 °C, and 70% humidity, 12 hour light–dark cycle). Vials were changed every 2 ~ 3 days and dead flies were counted. Experiments were repeated at least three times, with 100 ~ 150 flies examined for each genotype (Iijima et al., 2004). In the survival curves, the x-axis "age (days)" refers to the time after adult flies have eclosed from the pupae.

2.2.2. Climbing assay

Briefly, 20 flies were placed in a plastic vial and gently tapped to the bottom. The number of flies at the top of the vial was counted after 18 seconds of climbing under red light (Kodak, GBX-2, Safelight Filter). Data shown here represent results from a population of flies tested serially for 50 days, recorded every 5 days. The experiments were repeated at least three times.

2.2.3. Two choice tasting tests (Tanimura et al., 1988)

Flies were fed on sucrose solution soaked in Whatman paper for 2 h and were then starved for 20 h with only water. A blue dye − brilliant blue FCF ($C_{37}H_{34}O_9SNa$) and a red dye − acid red ($C_{27}H_{29}O_7N_2Na$), were used as internal markers of intake, as they were neither toxic nor metabolized at the test conditions. Sugar solution or water, mixed with either dye, was made up in 1% agar and applied to the wells of micro test plates. The wells in the plate were alternately filled with sugar solutions or water, each marked with the blue or red dye. Forty to fifty flies were introduced to the plate and fed for 2 hours at 25 °C in the dark before they were killed by freezing. Flies might have four abdominal colors, i.e. blue (B), red (R), mixed (M) and uncolored. Tests were counted meaningful if the uncolored flies were less than 5%. In the test between water and sucrose, the preference index (PI) of sucrose was expressed as the percentage of $[N_R + N_M/2]/[N_B + N_R + N_M]$, when water was marked red, and vice versa.

2.2.4. Pavlovian learning *in* Drosophila

We adopted the olfactory-avoidance classical (Pavlovian) conditioning protocol (Tully and Quinn, 1985), a standard method, to assess the learning and memory abilities. Flies were trained by exposure to electroshock paired with one odor (octanol or methylcyclohexanol) for 60 seconds and subsequent exposure to a second odor without electroshock for 60 seconds. After training, learning was immediately measured by allowing flies to choose between the two odors for 120 seconds. Before the assay, absolute olfactory acuity and shock reactivity were quantified. The PI was calculated by subtracting the number of flies making the

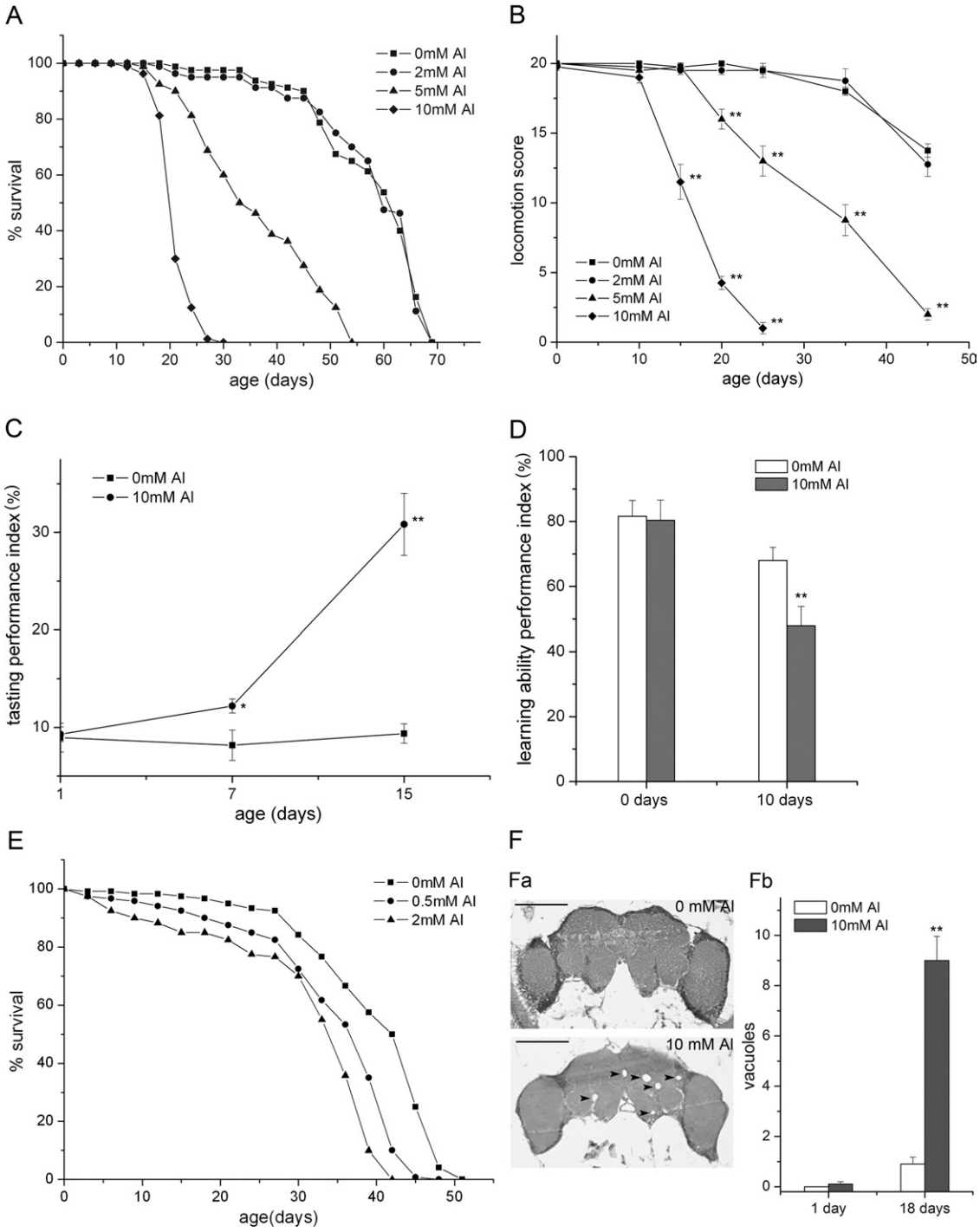

Fig. 1. Al exposure causes neurological damage. (A) Lifespan shortening because of Al exposure. 10 and 5 mM Al dramatically reduced the lifespans of the testing groups, log-rank, $p < 0.05$. (B) Al induces locomotion defects in flies. A high dosage exposure (10 mM) led to severe movement defect compared with the control group. Data are presented as means ± SEM (n = 4). (C) Al affects tasting behaviors, assayed by the Two-Choice Tasting Test. Tasting defects, indicated by tasting performance index; imply probable sensor neuron damage after Al exposure. 10 millimolar Al was used in the test. Higher scores reflect reduced tasting abilities. Significant difference was observed after 7-days feeding and the phenotype substantially more severe after 15 days. Data are presented as means ± SEM (n = 4). (D) Al affects learning-ability, as assayed by the Pavlovian-Learning-Ability Test. After 10-days feeding, the learning score of Al treated group was significantly lower than the no-treatment control group. Data are presented as means ± SEM (n ≥ 7). (E) Lower concentrations of Al can reduce lifespan when Al treatment starts from the early larva stage. Obvious reduction of lifespan could be observed at 0.5 and 2 mM of Al. 0 millimolar Al *vs.* 2 or 0.5 mM Al, log-rank, $p < 0.10$. Experiments were performed twice and the results were reproducible. Flies were reared at 29 °C in this experiment. The x-axis refers the age of adult flies. (F) Histological examinations confirm neurological damages inflicted by Al treatment (Fa). Horizontal paraffin head sections of 18-day-old, 10 mM Al treated flies and the control group, stained with H and E. The arrows indicate the neurodegenerative bubbles. Scales, 50 μm (Fb). statistic results for the histological examinations. Data are presented as means ± SEM (n ≥ 9). *$p < 0.05$, and **$p < 0.005$, two-tailed Student's *t*-test. x-axis represents the days after eclosion (adult fly age).

incorrect choice from those making the correct one, dividing by the total number of flies, and multiplying by 100. To avoid odor-avoidance biases, we calculate the PI of each single *n* by taking an average performance of two groups of flies: one group trained with the electroshock being OCT and the other with the electroshock being MCH.

2.3. Histological examination

Fly brains were fixed in PBS+ 4% formaldehyde overnight at room temperature, dehydrated, embedded in paraffin and cut (4 μm thickness) as described (Wu and Li, 2009). Sections were stained with Mayer's H&E and examined under a Nikon *Eclipes* 80i microscope attached to a Nikon DXM 1200F digital camera. Continuous sections were analyzed and the numbers of vacuoles in each brain were recorded. At least 10 brains were counted for each treatment.

2.4. Superoxide dismutase (SOD) and aconitase activity assays

2.4.1. SOD activity gels

For analysis of SOD activity by nitro blue tetrazolium (NBT) (Culotta et al., 1997), samples were resuspended in 0.5 ml of lysis buffer containing 10 mM sodium phosphate (pH 7.8), 1.0 mM EDTA, 0.1% Triton, 20 mg/ml leupeptin, 10 mg/ml pepstatin, 5% glycerol, and 1.0 mM phenylmethylsulfonyl fluoride, and applied directly without boiling to a nondenaturing 12% polyacrylamide gel. Following electrophoresis, the gel was stained in a solution containing 50 mM potassium phosphate (pH 7.8), 275 mg/ml NBT, 65 mg/ml riboflavin and 3.2 ml/ml TEMED. The intensity of bands was quantitated using ImageJ (National Institutes of Health, USA).

2.4.2. Aconitase assay

Aconitase activity was analyzed by the cis-aconitate method (Henson and Cleland, 1967). The enzyme activity was measured by the disappearance rate of cis-aconitate. Protein samples were added to 0.28 ml of aconitase buffer (20 mM Tris-HCl, 100 mM NaCl, 0.2 mM cis-aconitate, pH 7.2) and the decrease in absorbance at 240 nm was followed over time in a cuvette with a pathlength of 1 cm.

2.5. Mitochondria isolation and ROS measurement

Fly mitochondria were isolated using the standard method as described previously (Miwa et al., 2003). Generally, after crushed, cellular fragments were removed by two times 1,000 g centrifugation followed by two times 10,000 g centrifugation to obtain the mitochondria pellet. The mitochondria thus obtained are a crude fraction, but free of cytosol proteins as assayed by SOD activity assays. ROS of fly mitochondria was assayed with the DCFH (Dichlorfluorescein) (Cathcart et al., 1983), which is sensitive H_2O_2 and its derivative, such as ·OH, and DHE (Dihydroethidium) method, which is mostly used to detect $\cdot O_2^-$. Signals were monitored by Fluoroscan Ascent (Thermo Electron, Corp., USA).

2.6. Metal content assay

Newly eclosed flies were reared on normal food or food supplemented with compounds as noted. About 500 adults aged 18–20 days were collected, weighed and dissolved in 1 ml 65% HNO_3 (Sinopharm Chemical Reagent, Co. Ltd, China), boiled in 100 °C water bath for 10 minutes and diluted to 10 ml final for metal content analysis with inductively coupled plasma optical emission spectrometry (ICP-OES) (IRIS Intrepid II XSP, Thermo Electron Corporation, USA).

2.7. RNA extraction and RT-PCR

Total RNA was extracted from larvae or male adults using the TRIzol® Reagent (Invitrogen, USA). cDNA was transcribed from 1 μg total RNA with Superscript™ II reverse transcriptase (Invitrogen) according to the manufacturer's instructions. Semiquantitative RT-PCR was performed using primers to amplify partial regions of *rp49* (Wu and Li, 2009) and *Fer1* respectively. Intensity of gel bands was quantitated using ImageJ densitometry.

Primers used for RT-PCR are listed below: 5=GCACCAAGCACTTCATCC-3=(*rp49* forward); 5=CGATCTCGCCGCAGTAAA-3= (*rp49* reverse); 5=CAGGAGTGGACCGATGGT-3= (*FER1HCH* forward); 5=GGTCTTGTCGAACAGGAACT-3=(*FER1HCH* reverse).

2.8. Statistical analysis

The *p*-values were calculated using the Student's *t*-test ($*p < 0.05$; $**p < 0.005$). Survival curves were analyzed by the Kaplan and Meier method, and a log-rank was stated.

3. Results

3.1. Al treatment reduces Drosophila lifespan and results neurodegeneration in the brain

To evaluate the toxicity of Al to flies, different dosages of this metal were fed to newly eclosed flies. The survival curves and locomotion abilities were recorded. Dosage dependent toxicity was observed in both the lifespan and locomotion assays (Fig. 1A and B). While low concentration (2 mM) of Al feeding did not affect the lifespan and climbing ability compared with the normal food control (0 mM), median (5 mM) or high concentration (10 mM) of Al led to dramatically reduced median lifespan (34 days for 5 mM Al, 21 days for 10 mM Al, v. 61 days for 0 mM Al) and climbing ability (the age with 50% reduced ability was 15 days for 10 mM Al, compared with 50 days for 2 mM Al or 0 mM Al). Two neurological specific assays, the two-Choice Tasting Test for the sensor neurons and Pavlovian-Learning-Ability Test for the central nervous system, were additionally performed to examine the extent of damage to neurological functions in Al-treated flies. In both mentioned

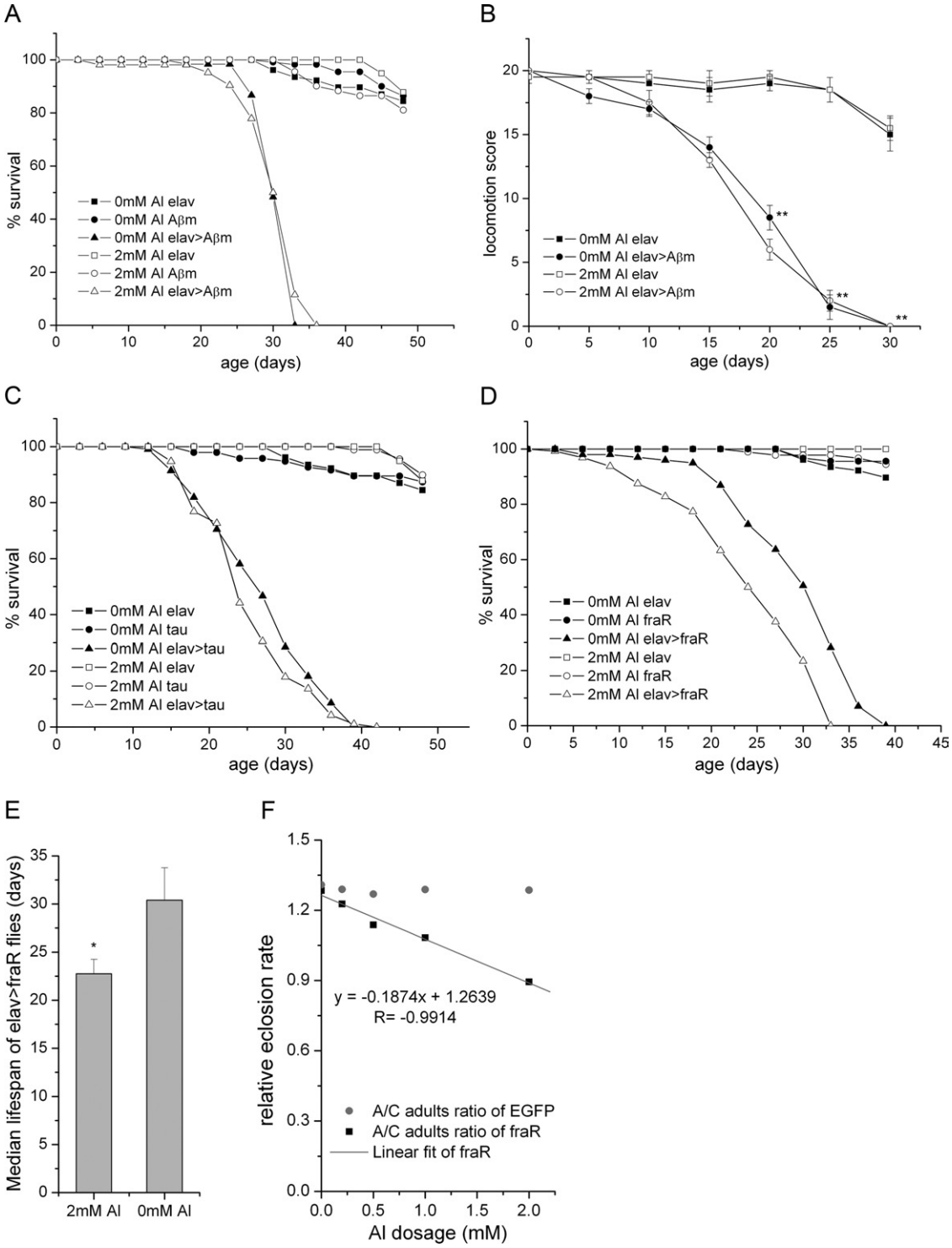

Fig. 2. Al does not interact with either *Drosophila* AD or tauopathy, but with Friedreich's ataxia. (A,B) Al toxicity in the *Drosophila* AD model. Al was not more toxic in the *Drosophila* AD model. Survival curve (A) and (B) locomotion ability (B). Data are presented as means ± SEM (n = 4) and compared with *elav-GAL4/+* flies. (C) Al toxicity in the *Drosophila* tauopathy model. Tauopathy flies also displayed no heightened vulnerability to Al toxicity in the survival assay. (D,E,F) Al toxicity in the *Drosophila* Friedreich's ataxia (*dfh*-RNAi) model. Synergistic effect was observed in the lifespan assay at low concentrations of Al which would not cause noticeable effect in normal flies. Survival curve (D), half-life comparison (E) and the relative eclosion (F). For the survival curve (D), 0 mM Al elav > fraR *vs.* 2 mM Al elav > fraR, log-rank, $p < 0.10$. The experiment was repeated (not shown here) and the results were similar. In the eclosion assay (F), *actin-GAL4/Cyo* was crossed to *UAS-dfh-RNAi* or *UAS-EGFP* (control), and the relative eclosion rate of *dfh*-RNAi flies (*actin-GAL4/UAS-dfh-RNAi*) to *Cyo* flies (*Cyo/UAS-dfh-RNAi*) under various Al concentrations was compared with that of *UAS-EGFP* flies (*actin-GAL4/UAS-EGFP*) to *Cyo* (*Cyo/UAS-EGFP*). *$p < 0.05$, and **$p < 0.005$, two-tailed Student's *t*-test. Days on x-axis are the age after eclosion.

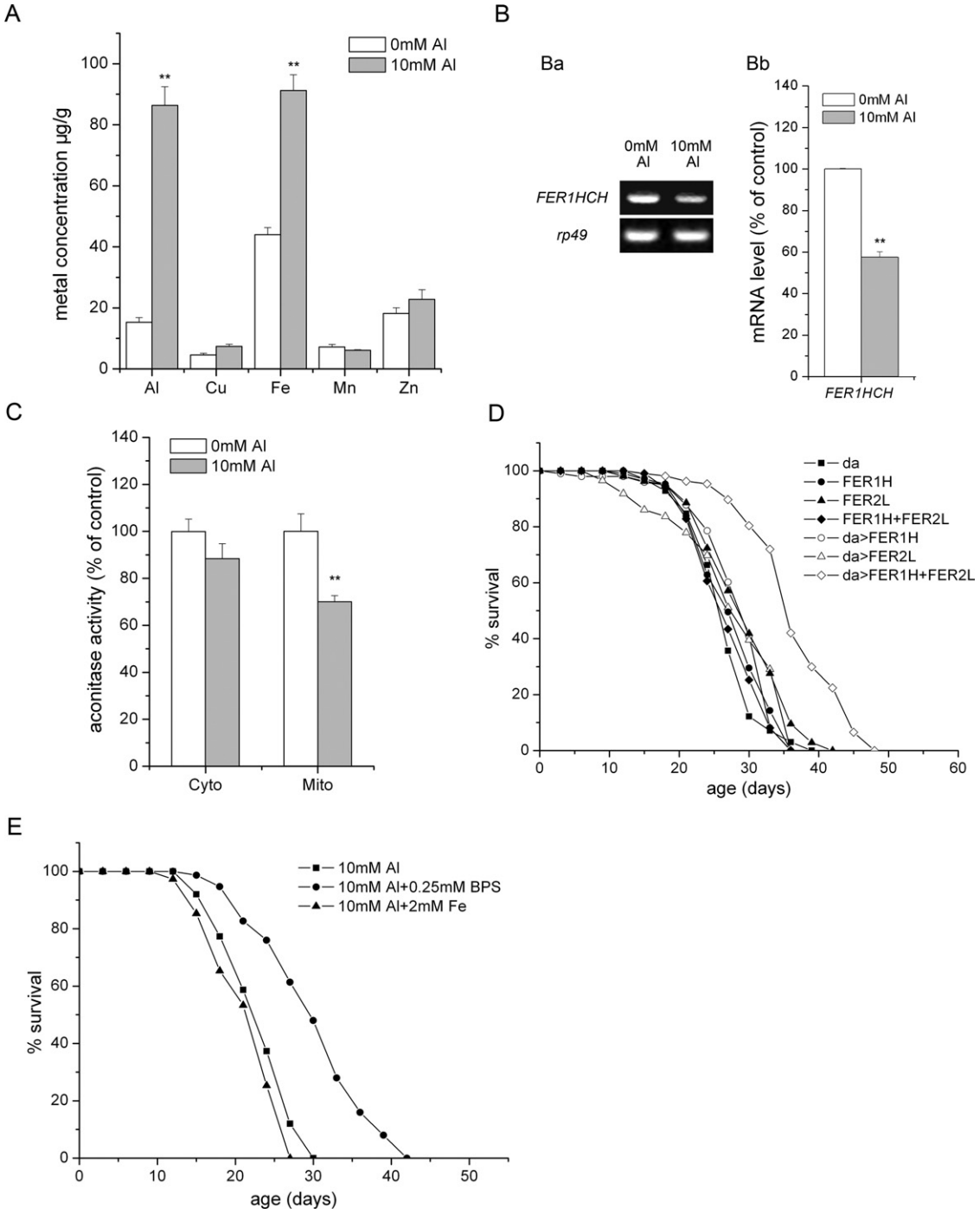

Fig. 3. Al disturbs iron homeostasis. (A) Al exposure (10 mM Al, 18 ~ 20 days) resulted Fe accumulation. (B) Al treatment led to the decrease of *ferritin* mRNA level. (Ba) Expression of two different *ferritin* genes was examined by semiquantitative PCR. *FER1HCH* expression was decreased compared with the control group. Flies were treated with 10 mM Al after eclosion for 18 ~ 20 days before the assay. (Bb) Statistical analysis of Aa. Data are presented as means ± SEM (n = 3). (C) Aconitase activity after Al exposure. Al resulted reduction of mitochondria aconitase activity, whereas cytosolic aconitase activity was not significantly changed. Al treatment started after eclosion and lasted for 10 days. Data are presented as means ± SEM (n ≥ 3). (D) Suppression of Al toxicity by ferritin overexpression. Ferritin overexpression could suppress Al toxicity *in vivo*. Fer1HCH (median lifespan: 28 days) or Fer2LCH (median lifespan: 27 days) alone was not beneficial to the flies, but coexpression was (median lifespan: 36 days) in the presence of 10 mM Al. Log-rank, $p < 0.05$. da: *da*-GAL4/+ control flies; FER1H: UAS-FER1HCH/+; FER2L: UAS-FER2L/+; da>: da-GAL4 drived expression, for instance, da > FER1H stands for *da-GAL4/UAS-FER1HCH*. (E) Reduction of Al toxicity by Fe chelator. Fe chelator (0.25 mM BPS) ameliorated but exogenous Fe did not enhance Al damage. Log-rank, $p < 0.05$. Higher BPS level (such as 0.5 mM BPS) resulted Fe shortage to flies, while 0.1 mM BPS was less effective than 0.25 mM in relieving Al toxicity. *$p < 0.05$, and **$p < 0.005$, two-tailed Student's *t*-test.

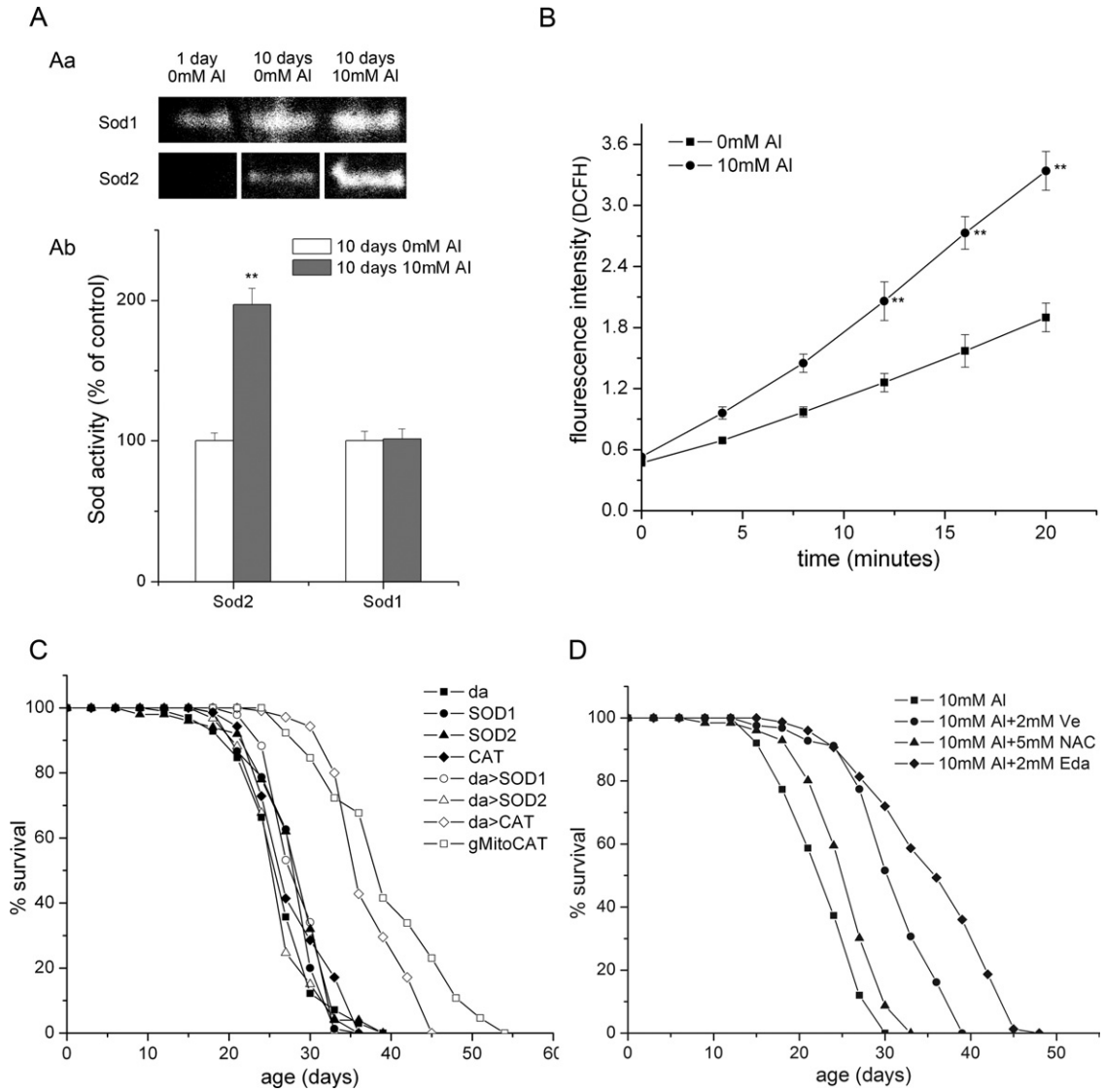

Fig. 4. Mitochondria ROS greatly contributes to Al neurotoxicity. (A) SOD activity after Al treatment. (Aa) Mitochondria SOD2 level, assayed in native gels, was significantly increased in Al-treated flies. (Ab) Statistic analysis for Aa. Data are presented as means ± SEM (n = 3). (B) ROS production in Al-treated flies mitochondria. ROS was monitored by DCF fluorescence intensity in the isolated mitochondria. Mitochondria from Al-fed flies generated much more ROS than the control. Data are presented as means ± SEM (n = 3). (C) Suppression of Al toxicity by catalase. Flies with extra expression of catalase, but not SOD1 or SOD2, were much more resistant to the toxicity of Al (10 mM). Control − no exogenous catalase transgene (median lifespan: 25 days); catalase flies (median lifespan: 35 days); mitochondria catalase flies (median lifespan: 40 days). Lifespan comparison between the control and catalase flies, log-rank, $p < 0.05$. (D) Reduction of Al-induced toxicity by ROS chemical scavengers. Lifespans of Al-treated flies could be elongated by the addition of ROS scavengers. Hydrophilic scavenger NAC (median lifespan: 22.5 days) showed little benefit to the Al-fed flies (median lifespan: 25 days), however, the hydrophobic Vitamin E (median lifespan: 32.5 days) and Edaravone (median lifespan: 37.5 days) both exhibited significant rescuing effect. For lifespans comparison, log-rank, $p < 0.05$. For the other analyses (in A and B), *$p < 0.05$, and **$p < 0.005$, two-tailed Student's t-test.

assays, Al-treated flies exhibited significantly decreased capabilities when compared with their nonfeeding congeners (0 mM Al). In the tasting assay, 15-day-old flies showed a dramatic loss of ability to distinguish sugar from water (Fig. 1C); in the Pavlovian-Learning-Ability Test, the learning ability of 10-day-old flies was significantly lower in the Al-treated group than that of the flies in the normal food control group (0 mM Al) (Fig. 1D).

More pronounced Al effect could be observed when Al feeding was started from freshly hatched larvae onwards, instead of started from the adult stage. When Al exposure persisted throughout the lifespan 0.5 mM Al could inflict significant damage to the flies (Fig. 1E), whereas as a comparison, no obvious drop of longevity was observed when 2 mM or less Al was fed starting at the adult stage (Fig. 1A).

Histological examination of Al-treated flies' brains confirmed the observations from the behavioral assays: degenerative vacuoles were found in Al-treated flies but not the homochronous normal control (0 mM Al) (Fig. 1Fa). Sta-

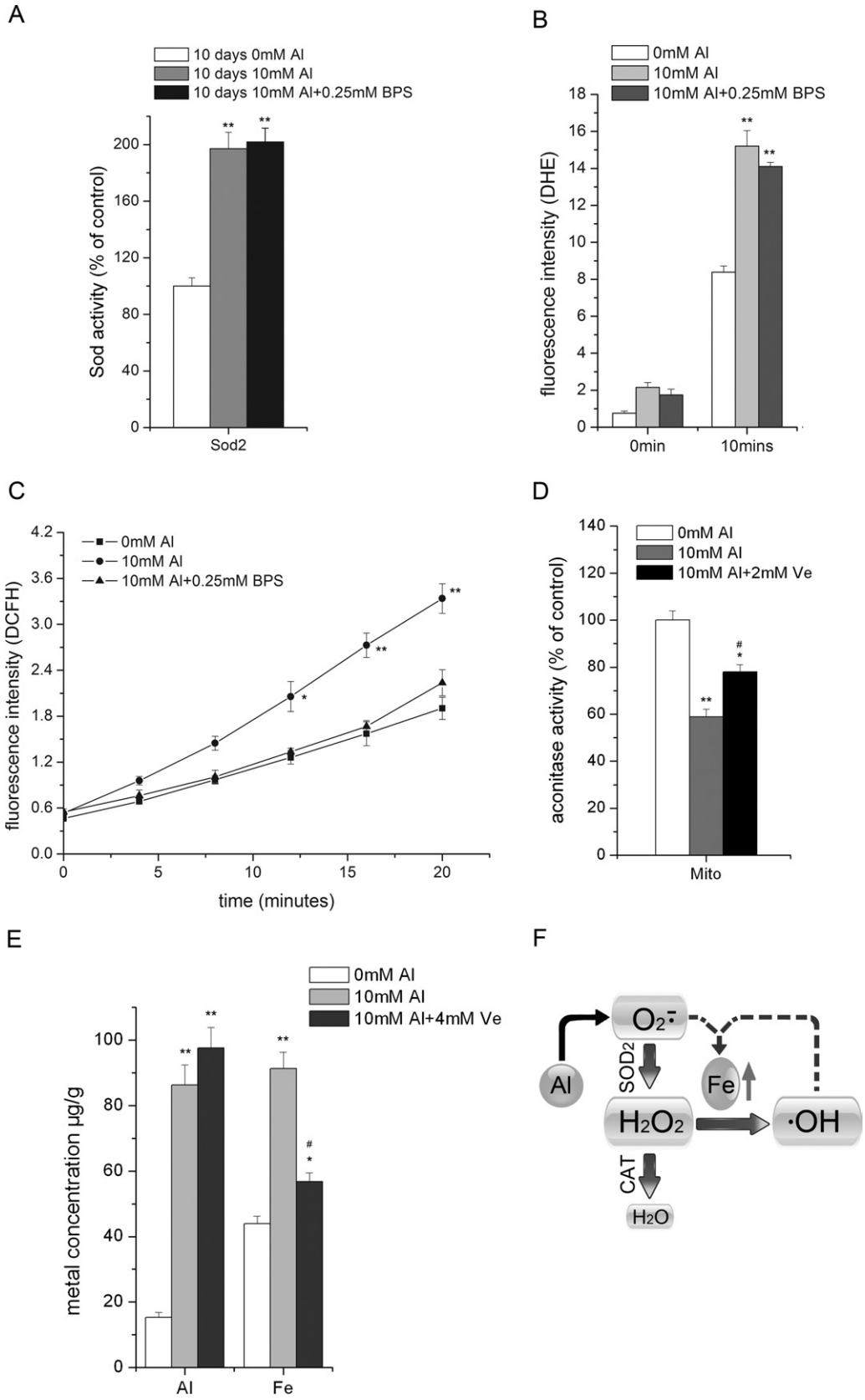

Fig. 5. Al-caused iron dyshomeostasis is mediated by mitochondria ROS generation. Fe chelation reduced other ROS, but not $\cdot O_2^-$ production, whereas ROS scavengers partially normalized iron homeostasis. (A) SOD2 activity in BPS-treated Al-fed flies. SOD2 activity was not changed when treated with BPS in

tistical analysis of the vacuole numbers through continuous sections revealed a dramatic increase of brain cell death in Al-treated flies (Fig. 1Fb).

Together, Al treatment could result in neuronal toxicities. A broad spectrum of behavioral and physiological abnormalities was observed in Al-treated flies.

3.2. Al toxicity is synergistic with that of frataxin mutation but not with Aβ or Tau

The relevance of Al to AD is a controversial topic. Because Al causes memory loss, we investigated how Al exposure would alter the course of disease in AD or Tau fly models. In the AD model, we tested overexpression of the Arctic mutation of human β-amyloid 42 peptide (Aβ42Arc, with E22G substitution), which causes early onset familial AD (EOFAD) (Iijima et al., 2008). In the fly, overexpression of Aβ42Arc led to a more severe phenotype than the normal Aβ42. In the Ta'u model, we used *tauR406W* (Wittmann et al., 2001). Expression of these genes was made possible through the use of the GAL4/UAS bipartite expression system, in which the transgenes are directed by UAS binding sites and can be activated by the UAS binding factor Gal4.

We treated these adult flies with 2 mM Al, a dosage that showed little damaging effect to normal flies. No dramatically reduced lifespan was observed in Aβ42Arc mutant overexpression flies (Fig. 2A). The progressive locomotion defect of flies expressing Aβ42Arc was also monitored: 2 mM of Al did not accelerate the deteriorating process (Fig. 2B). Similarly, under this concentration Al toxicity was not noticed in the flies with expression of the human mutant tau protein either (Fig. 2C).

We additionally tested another *Drosophila* model, *dfh*-RNAi, for a rare human neurodegenerative disease Friedreich's ataxia (Llorens et al., 2007). Interestingly, chronic exposure to low amounts of Al, while caused no obvious harmful effect on normal and AD or Tau adult flies, resulted noticeably detrimental effect on the *dfh*-RNAi flies (Fig. 2D). The half-life of *dfh*-RNAi flies fed with 2 mM Al, unlike that of the AD or Tau flies, was significantly reduced compared with the control (0 mM Al group) (Fig. 2E). In addition, when we treated *dfh*-RNAi flies with Al from the larva stage, developmental retardation was obvious and much severer than the wild type (data not shown). We quantitatively gauged this relative sensitivity to Al by measuring the relative eclosion rate of *dfh*-RNAi vs. control (EGFP flies). We considered that if *dfh*-RNAi flies are more vulnerable to Al toxicity, under Al treatment a lower relative eclosion of *dfh*-RNAi is expected. Indeed, the relative eclosion of *dfh*-RNAi was linearly, but inversely, related to Al levels (Fig. 2F). These findings suggest that Al toxicity acts in a different pathway from those leading to Aβ42 and Tau toxicity, but may share a similar mechanism with that of *frataxin* mutation.

3.3. Al exposure results in iron dyshomeostasis and ROS production

Metal dyshomeostasis correlates with the initiation and progress of various human neurodegenerative diseases (Hayflick, 2006; Yokel, 2006), although whether this correlation is a causing effect or not remains largely unknown. Metal dyshomeostasis has also been observed in Al-treated cells and Al-induced animal models (Bondy and Kirstein, 1996; Vasudevaraju et al., 2008). We thus analyzed the metal content in Al-treated flies (Fig. 3A). Amazingly, Al treatment led to a dramatic increase of Fe level (in addition to Al), while leaving that of other metals much less significantly affected. Semiquantitative RT-PCR of *ferritin* gene (*FER1HCH*), a marker of Fe bioavailability, was performed to verify that iron dyshomeostasis did occur in these flies. Contrary to our thinking, expression of *FER1HCH* was reduced in the Al-treated flies, indicating though total Fe level was elevated, a general deficiency of bioavailable Fe existed in these cells (Fig. 3B). The aconitase activity, which also indirectly monitors the iron availability (Henson and Cleland, 1967), was significantly decreased in the mitochondria, but only marginally and statistically insignificantly reduced in the cytosol (Fig. 3C), implying a primary mitochondrial effect of Al damage. These pieces of data suggested that Al treatment resulted in the cell sensing a lack of Fe, and the Fe accumulation was probably a feedback or compensating result of this "deficiency".

Increase of Fe will likely exacerbate ROS generation. Accordingly, we next studied ROS production in Al-treated flies. As a first indicator, we analyzed SOD activities (SOD1 and SOD2) since they often respond to superoxide levels. Interestingly, the mitochondrial SOD2 activity was dramatically increased by Al exposure, while that of SOD1, a cytosolic SOD, remained relatively unaffected (Fig. 4A). We subsequently measured mitochondrial H_2O_2 generation with DCFH using isolated mitochondria from 10-day-old flies. As shown in Fig. 4B, mitochondrial ROS generation in

Al-fed flies. Flies were 10 days after eclosion. Data are presented as means ± SEM (n = 3). (B,C) ROS production in BPS-treated Al-fed flies. Flies were 10 days after eclosion. Using DHE as the indicator to monitor the mitochondria ROS condition, it appeared that superoxide generation is not changed by BPS (B). DCFH, an indicator sensitive to peroxide, indicated that the presumed peroxide production from Al was significantly reduced by BPS treatment (C). Data are presented as means ± SEM (n = 3). (D) Mitochondria aconitase activity after antioxidant treatment. Mitochondria aconitase activity was partially restored with antioxidant treatment. Vitamin E was used. Flies were 10 days after eclosion. Data are presented as means ± SEM (n = 3). (E) Fe accumulation after antioxidant treatment. Fe accumulation could be greatly reversed by 4-mM Vitamin E treatment. Transition metal concentrations were measured by ICP-MS. Data are presented as means ± SEM (n = 3). (F) A model to explain the cycling reaction of ROS and Fe induced by Al. * or #$p < 0.05$, and **$p < 0.005$, two-tailed Student's *t*-test. * and ** are compared with 0 mM Al, and # compared with 10 mM Al group.

the Al-treated flies was much higher than the nontreatment flies.

In summary, iron metabolism and ROS production were significantly affected in Al-treated flies. Notably, similar phenomena were also reported in *Drosophila* frataxin homolog or *dfh* mutant flies (Anderson et al., 2005; Kondapalli et al., 2008; Llorens et al., 2007).

3.4. Mitochondrial ROS and iron accumulation contributes to Al neurotoxicity

To investigate the functional aspect of this iron accumulation in relevance to Al toxicity, we tried to overexpress ferritin genes to ameliorate the possible free Fe damage. Simultaneous expression of both Fer1HCH and Fer2LCH greatly reduced Al toxicity, whereas neither Fer1HCH nor Fer2LCH alone was beneficial (Fig. 3D). Consistent with this finding, 0.25 mM Fe chelator bathophenanthroline disulfonic acid (BPS) could significantly reduce the toxicity of Al *in vivo* and dramatically elongate the median lifespan of flies on high dosage Al diet (Fig. 3E). As a control, the same concentration of BPS did not seem to benefit flies on normal food, and if anything, slightly reduced the life span of these flies (data not shown). Higher BPS levels (such as 0.5 mM) were also tested but were found harmful to even normal flies. By contrast, additional Fe (2 mM) did not enhance the toxicity of Al, suggesting that the Fe level in the normal food was sufficiently high already or alternatively, excess exogenous Fe addition would not significantly alter the Fe level in the subcellular organelle where Al acts.

To ascertain the significance of ROS production in Al toxicity, antioxidases SOD1, SOD2 and catalase were expressed in flies via UAS/GAL4 system. An engineered mitochondria-targeted catalase (mito-CAT) under the control of its endogenous genomic promoter (Anderson et al., 2008) was also tested. Ubiquitous expression of antioxidases driven by *da-GAL4* caused differential effects in flies on Al diet: overexpression of SOD1 and SOD2 failed to show any improvement compared with the control flies, whereas expression of catalase or the engineered mitochondria-targeted catalase (mito-CAT) benefited the host significantly (Fig. 4C). Consistently, antioxidants could also mitigate Al toxicity. Hydrophobic antioxidants 3-methyl-1-phenyl-2-pyrazoline-5-one (Edaravone, Simcere Co., China) and vitamin E could both significantly elongate the median lifespan of Al-treated flies, but the hydrophilic compound N-Acetyl-Cysteine (NAC) could not (Fig. 4D).

Since BPS and ROS scavengers could both alleviate Al toxicity, we examined the relationship between Fe dyshomeostasis and ROS production from Al treatment. Intriguingly, the increased SOD2 level was not altered by BPS addition (Fig. 5A). Measurement of the ROS level with DHE and DCFH obtained different results (Fig. 5B and 5C). When DHE was used, BPS treatment failed to decrease significantly the fluorescence signal, whereas when DCFH was used, a great reduction of the fluorescence signal was observed. We interpret this apparent paradox by that DHE and DCFH detect different kinds of ROS: DHE is mostly used to detect $\cdot O_2^-$, while DCFH for H_2O_2 and its derivative, such as ·OH. It is possible that BPS altered the level of other types of ROS but not much that of $\cdot O_2^-$. On the other side, reducing ROS by feeding with ROS scavenger could significantly normalize the Fe level (Fig. 5E) and the mitochondria aconitase activity (Fig. 5D). It therefore appears that $\cdot O_2^-$ production because of Al treatment originated first, which in turn caused iron dyshomeostasis and the increased Fe accelerated further other ROS production (Fig. 5F. See Discussion for details).

4. Discussion

Here, we demonstrated the neurotoxicity of Al in a *Drosophila* model. Increased mitochondrial ROS production and iron dyshomeostasis were observed in Al-treated flies. With the help of genetic and pharmacological methods to ameliorate ROS or iron accumulation, we provided strong functional evidence to link aluminum toxicity with iron and ROS accumulation.

Although Al causes $\cdot O_2^-$ production (Figs 4A, 5A, 5B) (Kumar et al., 2009), the primary damage because of Al treatment appears not from $\cdot O_2^-$ because BPS addition can alleviate Al toxicity, but would not significantly reduce $\cdot O_2^-$ level. In addition, increased expression of catalase but not SOD1 or SOD2 suppresses Al toxicity. The elevated SOD2 but not SOD1 activity may be a physiological response to the increased mitochondrial $\cdot O_2^-$ level by Al, whereas the heightened $\cdot O_2^-$ level in Al-treated flies could arise from interference of Al with the electron transport chain, as suggested before (Dua and Gill, 2004; Kumar et al., 2008).

We initially considered Al might directly alter Fe homeostasis to exert its toxicity. However, although iron chelator (BPS) and scavengers can both mitigate Al toxicity, BPS did not disturb the mitochondrial $\cdot O_2^-$ production, whereas ROS scavengers could significantly ameliorate Al induced Fe accumulation. Therefore we believe that the most proximal effect of Al is to generate $\cdot O_2^-$, although its toxicity is finally mediated mostly by Fe and $\cdot OH/H_2O_2$ accumulation. A model to explain Al toxicity is shown in Fig. 5F: Al interferes with the mitochondrial electron transport chain (ETC) and as a result, generating an acute increase of $\cdot O_2^-$ level. $\cdot O_2^-$ is then converted to H_2O_2, which jointly with ·OH interacts with Fe and starts a vicious cycle, leading to more ROS and Fe accumulation, ultimately damaging mitochondrial functions. Hence, the Fe accumulation observed is likely a secondary effect, mostly due to the cellular sensing of iron deficiency because of $\cdot O_2^-$ caused damage of the iron sulfur clusters, a critical component of iron homeostasis controller IRP. This model for Al action explains why BPS addition reduces ROS formation as detected by DCFH but not by DHE, and ROS scavengers not

only reduce ROS level but also iron accumulation (due to the broken "vicious ROS-Fe cycle"). The suppression of Al toxicity by both normally cytosol-localized catalase and mitochondrial targeted catalase (mito-CAT) may reflect the fact that H_2O_2 is a diffusible factor (Waghray et al., 2005). In a previous report, it was shown that Al could to some extent antagonize Fe-induced IRP2 oxidation *in vitro*, stabilizing IRP2 protein (Yamanaka et al., 1999). However, in our experiments we found ROS scavenger (vitamin E) could dramatically reduce Al induced Fe accumulation. We therefore believe Fe accumulation after Al treatment largely arises from ROS damage although some direct effect of Al on Fe homeostasis cannot be excluded.

Our scheme of Al action is to some extent reminiscent of what has been seen for frataxin mutation. In frataxin mutants, because of mitochondrial iron dyshomeostasis, increased Fe and ROS in the mitochondria were also reported (Anderson et al., 2008; Wong et al., 1999). Consistently, Al seems more toxic in a fly model of Friedreich's ataxia, suggesting Friedreich's ataxia patients may be more vulnerable to Al exposure.

The controversy whether Al has a direct link to common human neurodegenerative diseases, such as AD, has been debated for decades. Conflicting data exist in the literature (Mizoroki et al., 2007; Savory and Ghribi, 2007; Savory et al., 2006). Although it is relatively certain that Al displays multifaceted and complicated neurotoxicity at low dosages, some of which appears relevant to AD disease, there is still no direct evidence to link Al as a high risk factor for AD as happening in the general population. In *Drosophila*, chronic Al exposure can also cause the severe neurological disorders, including locomotion-ability loss, learning ability loss and early death in adults, and neurodegenerative vacuoles in aged Al treated flies. However, the pattern of neurodegeneration induced by Al is not consistent with AD model: the vacuoles in *Drosophila* AD Model is predominantly found in cell body regions (Iijima et al., 2004; Iijima et al., 2008), while neurodegeneration of Al-treated flies mainly resides in the neuropil region (Fig. 1F). Further, neither human β-amyloid (both wild type and mutant proteins) nor tau overexpression flies exhibited no less and no more sensitivity to Al. Taken together, it seems that Al toxicity markedly diverges from that as induced by β-amyloid or Tau.

Disclosure statement

The authors disclose that there are no actual or potential conflicts of interest.

Acknowledgements

This work was supported by National Scientific Foundation of China [no. 30688001 and no. 30528004], and the National Basic Research Program of China [no. 2005CB522503]. We thank Dr. A. Hilliker, Dr. Molto and Dr. F. Missirlis for transgenic fly stocks (see Material and methods). A generous help was provided by YC. Shuai in the fly memory/learning assay.

References

Anderson, P.R., Kirby, K., Hilliker, A.J., Phillips, J.P., 2005. RNAi-mediated suppression of the mitochondrial iron chaperone, frataxin, in Drosophila. Hum. Mol. Genet. 14, 3397–3405.

Anderson, P.R., Kirby, K., Orr, W.C., Hilliker, A.J., Phillips, J.P., 2008. Hydrogen peroxide scavenging rescues frataxin deficiency in a Drosophila model of Friedreich's ataxia. Proc. Natl. Acad. Sci. U S A 105, 611–616.

Bertholf, R.L., Herman, M.M., Savory, J., Carpenter, R.M., Sturgill, B.C., Katsetos, C.D., Vandenberg, S.R., Wills, M.R., 1989. A long-term intravenous model of aluminum maltol toxicity in rabbits: tissue distribution, hepatic, renal, and neuronal cytoskeletal changes associated with systemic exposure. Toxicol. Appl. Pharmacol. 98, 58–74.

Bilen, J., Bonini, N.M., 2005. Drosophila as a model for human neurodegenerative disease. Annu. Rev. Genet. 39, 153–171.

Bondy, S.C., Kirstein, S., 1996. The promotion of iron-induced generation of reactive oxygen species in nerve tissue by aluminum. Mol. Chem. Neuropathol. 27, 185–194.

Cathcart, R., Schwiers, E., Ames, B.N., 1983. Detection of picomole levels of hydroperoxides using a fluorescent dichlorofluorescein assay. Anal. Biochem. 134, 111–116.

Culotta, V.C., Klomp, L.W., Strain, J., Casareno, R.L., Krems, B., Gitlin, J.D., 1997. The copper chaperone for superoxide dismutase. J. Biol. Chem. 272, 23469–23472.

Dobson, C.B., Day, J.P., King, S.J., Itzhaki, R.F., 1998. Location of aluminum and gallium in human neuroblastoma cells treated with metal-chelating agent complexes. Toxicol. Appl. Pharmacol. 152, 145–152.

Drago, D., Cavaliere, A., Mascetra, N., Ciavardelli, D., di Ilio, C., Zatta, P., Sensi, S.L., 2008. Aluminum modulates effects of beta amyloid(1–42) on neuronal calcium homeostasis and mitochondria functioning and is altered in a triple transgenic mouse model of Alzheimer's disease. Rejuvenation Res. 11, 861–871.

Dua, R., Gill, K.D., 2004. Effect of aluminum phosphide exposure on kinetic properties of cytochrome oxidase and mitochondrial energy metabolism in rat brain. Biochim. Biophys. Acta 1674, 4–11.

Hayflick, S.J., 2006. Neurodegeneration with brain iron accumulation: from genes to pathogenesis. Semin. Pediatr. Neurol. 13, 182–185.

Henson, C.P., Cleland, W.W., 1967. Purification and kinetic studies of beef liver cytoplasmic aconitase. J. Biol. Chem. 242, 3833–3838.

Iijima, K., Chiang, H.C., Hearn, S.A., Hakker, I., Gatt, A., Shenton, C., Granger, L., Leung, A., Iijima-Ando, K., Zhong, Y., 2008. Abeta42 mutants with different aggregation profiles induce distinct pathologies in Drosophila. PLoS ONE 3, e1703.

Iijima, K., Liu, H.P., Chiang, A.S., Hearn, S.A., Konsolaki, M., Zhong, Y., 2004. Dissecting the pathological effects of human. Abeta 40 and Abeta42 in Drosophila: a potential model for Alzheimer's disease. Proc Natl Acad Sci U S A 101(17), 6,623–628.

Karlik, S.J., Eichhorn, G.L., Lewis, P.N., Crapper, D.R., 1980. Interaction of aluminum species with deoxyribonucleic acid. Biochemistry 19, 5991–5998.

Khanna, P., Nehru, B., 2007. Antioxidant enzymatic system in neuronal and glial cells enriched fractions of rat brain after aluminum exposure. Cell. Mol. Neurobiol. 27, 959–969.

Kihira, T., Yoshida, S., Kondo, T., Yase, Y., Ono, S., 2004. ALS-like skin changes in mice on a chronic low-Ca/Mg high-Al diet. J. Neurol. Sci. 219, 7–14.

Kim, Y., Olivi, L., Cheong, J.H., Maertens, A., Bressler, J.P., 2007. Aluminum stimulates uptake of non-transferrin bound iron and trans-

ferrin bound iron in human glial cells. Toxicol. Appl. Pharmacol. 220, 349–356.

Klatzo, I., Wisniewski, H., Streicher, E., 1965. Experimental Production of Neurofibrillary Degeneration. I. Light Microscopic Observations. J. Neuropathol. Exp. Neurol. 24, 187–199.

Kondapalli, K.C., Kok, N.M., Dancis, A., Stemmler, T.L., 2008. Drosophila frataxin: an iron chaperone during cellular Fe–S cluster bioassembly. Biochemistry 47, 6917–6927.

Kumar, V., Bal, A., Gill, K.D., 2008. Impairment of mitochondrial energy metabolism in different regions of rat brain following chronic exposure to aluminum. Brain Res. 1232, 94–103.

Kumar, V., Bal, A., Gill, K.D., 2009. Susceptibility of mitochondrial superoxide dismutase to aluminum induced oxidative damage. Toxicology 255, 117–123.

Lankoff, A., Banasik, A., Duma, A., Ochniak, E., Lisowska, H., Kuszewski, T., Gozdz, S., Wojcik, A., 2006. A comet assay study reveals that aluminum induces DNA damage and inhibits the repair of radiation-induced lesions in human peripheral blood lymphocytes. Toxicol. Lett. 161, 27–36.

Llorens, J.V., Navarro, J.A., Martinez-Sebastian, M.J., Baylies, M.K., Schneuwly, S., Botella, J.A., Molto, M.D., 2007. Causative role of oxidative stress in a Drosophila model of Friedreich ataxia. FASEB J. 21, 333–344.

Massie, H.R., Williams, T.R., Aiello, V.R., 1985. Excess dietary aluminum increases Drosophila's rate of aging. Gerontology 31, 309–314.

Middaugh, J., Hamel, R., Jean-Baptiste, G., Beriault, R., Chenier, D., Appanna, V.D., 2005. Aluminum triggers decreased aconitase activity via Fe–S cluster disruption and the overexpression of isocitrate dehydrogenase and isocitrate lyase: a metabolic network mediating cellular survival. J. Biol. Chem. 280, 3159–3165.

Missirlis, F., Kosmidis, S., Brody, T., Mavrakis, M., Holmberg, S., Odenwald, W.F., Skoulakis, E.M., Rouault, T.A., 2007. Homeostatic mechanisms for iron storage revealed by genetic manipulations and live imaging of Drosophila ferritin. Genetics 177, 89–100.

Miu, A.C., Benga, O., 2006. Aluminum and Alzheimer's disease: a new look. J. Alzheimers Dis. 10, 179–201.

Miwa, S., St-Pierre, J., Partridge, L., Brand, M.D., 2003. Superoxide and hydrogen peroxide production by Drosophila mitochondria. Free Radic. Biol. Med. 35, 938–948.

Mizoroki, T., Meshitsuka, S., Maeda, S., Murayama, M., Sahara, N., Takashima, A., 2007. Aluminum induces tau aggregation in vitro but not in vivo. J. Alzheimers Dis. 11, 419–427.

Oyanagi, K., 2005. The nature of the parkinsonism-dementia complex and amyotrophic lateral sclerosis of Guam and magnesium deficiency. Parkinsonism Relat. Disord. 11 suppl 1, S17–S23.

Savory, J., Ghribi, O., 2007. Can studies of aluminum toxicity in vivo and in vitro provide relevant information on the pathogenesis and etiology of Alzheimer's disease? J. Alzheimers Dis. 11, 429–430; [Discussion, 31–32].

Savory, J., Herman, M.M., Ghribi, O., 2006. Mechanisms of aluminum-induced neurodegeneration in animals: Implications for Alzheimer's disease. J. Alzheimers Dis. 10, 135–144.

Savory, J., Rao, J.K., Huang, Y., Letada, P.R., Herman, M.M., 1999. Age-related hippocampal changes in Bcl-2: Bax ratio, oxidative stress, redox-active iron and apoptosis associated with aluminum-induced neurodegeneration: increased susceptibility with aging. Neurotoxicology 20, 805–817.

Tanimura, T., Isono, K., Yamamoto, M.T., 1988. Taste Sensitivity to Trehalose and Its Alteration by Gene Dosage in Drosophila Melanogaster. Genetics 119, 399–406.

Tully, T., Quinn, W.G., 1985. Classical conditioning and retention in normal and mutant Drosophila melanogaster. J. Comp. Physiol. A 157(2), 263–77.

Vasudevaraju, P., Govindaraju, M., Palanisamy, A.P., Sambamurti, K., Rao, K.S., 2008. Molecular toxicity of aluminum in relation to neurodegeneration. Indian J. Med. Res. 128, 545–556.

Waghray, M., Cui, Z., Horowitz, J.C., Subramanian, I.M., Martinez, F.J., Toews, G.B., Thannickal, V.J., 2005. Hydrogen peroxide is a diffusible paracrine signal for the induction of epithelial cell death by activated myofibroblasts. FASEB J. 19, 854–856.

Walton, J.R., 2007. An aluminum-based rat model for Alzheimer's disease exhibits oxidative damage, inhibition of PP2A activity, hyperphosphorylated tau, and granulovacuolar degeneration. J. Inorg. Biochem. 101, 1275–1284.

Ward, R.J., Zhang, Y., Crichton, R.R., 2001. Aluminum toxicity and iron homeostasis. J. Inorg. Biochem. 87, 9–14.

Wittmann, C.W., Wszolek, M.F., Shulman, J.M., Salvaterra, P.M., Lewis, J., Hutton, M., Feany, M.B., 2001. Tauopathy in Drosophila: neurodegeneration without neurofibrillary tangles. Science 293, 711–714.

Wong, A., Yang, J., Cavadini, P., Gellera, C., Lonnerdal, B., Taroni, F., Cortopassi, G., 1999. The Friedreich's ataxia mutation confers cellular sensitivity to oxidant stress which is rescued by chelators of iron and calcium and inhibitors of apoptosis. Hum. Mol. Genet. 8, 425–430.

Wu, Z., Li, C., 2009. S. Lv In Zhou, B. Pantothenate kinase-associated neurodegeneration: insights from a Drosophila model. Hum Mol Genet 18(19), 3, 659–672.

Yamanaka, K., Minato, N., Iwai, K., 1999. Stabilization of iron regulatory protein 2, IRP2, by aluminum. FEBS Lett. 462, 216–220.

Yokel, R.A., 1989. Aluminum produces age related behavioral toxicity in the rabbit. Neurotoxicol. Teratol. 11, 237–242.

Yokel, R.A., 2006. Blood–brain barrier flux of aluminum, manganese, iron and other metals suspected to contribute to metal-induced neurodegeneration. J. Alzheimers Dis. 10, 223–253.